

See discussions, stats, and author profiles for this publication at: <https://www.researchgate.net/publication/7965174>

Thermodynamic study of sesamol, piperonyl alcohol, piperonylic acid and homopiperonylic acid: A combined experimental and theoretical investigation

ARTICLE in ORGANIC & BIOMOLECULAR CHEMISTRY · APRIL 2004

Impact Factor: 3.56 · DOI: 10.1039/b400107a · Source: PubMed

CITATIONS

12

READS

55

5 AUTHORS, INCLUDING:



Manuel J S Monte

University of Porto

115 PUBLICATIONS 1,342 CITATIONS

SEE PROFILE



Clara Sousa

University of Minho

42 PUBLICATIONS 182 CITATIONS

SEE PROFILE



Victor Morais

University of Porto

90 PUBLICATIONS 790 CITATIONS

SEE PROFILE

Thermodynamic study of sesamol, piperonyl alcohol, piperonylic acid and homopiperonylic acid: a combined experimental and theoretical investigation

M. Agostinha R. Matos,^{*a} Manuel J. S. Monte,^a Clara C. S. Sousa,^a Ana R. R. P. Almeida^a and Victor M. F. Morais^{a,b}

^a Centro de Investigação em Química, Departamento de Química, Faculdade de Ciências da Universidade do Porto, Rua do Campo Alegre, 687, P-4169-007 Porto, Portugal.

E-mail: marmatos@fc.up.pt

^b Instituto de Ciências Biomédicas Abel Salazar, Universidade do Porto, P-4099-003 Porto, Portugal

Received 6th January 2004, Accepted 26th January 2004

First published as an Advance Article on the web 23rd February 2004

The standard ($p^\circ = 0.1$ MPa) molar energies of combustion in oxygen, at $T = 298.15$ K, of four 1,3-benzodioxole derivatives (sesamol, piperonyl alcohol, piperonylic acid and homopiperonylic acid) were measured by static bomb calorimetry. The values of the standard molar enthalpies of sublimation, at $T = 298.15$ K, were derived from vapour pressure–temperature measurements using the Knudsen effusion technique. Combining these results the standard molar enthalpies of formation of the compounds, in the gas phase, at $T = 298.15$ K, have been calculated: sesamol (-325.7 ± 1.9) kJ mol⁻¹; piperonyl alcohol (-329.0 ± 2.0) kJ mol⁻¹; piperonylic acid (-528.9 ± 2.6) kJ mol⁻¹ and homopiperonylic acid (-544.5 ± 2.9) kJ mol⁻¹.

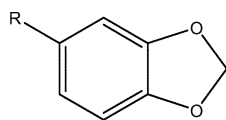
The most stable geometries of all the compounds were obtained using the density functional theory with the B3LYP functional and two basis sets: 6-31G** and 6-311G**. The nonplanarity of the molecules was analyzed in terms of the anomeric effect, which is believed to arise from the interaction between a nonbonded oxygen p orbital and the empty orbital σ^*_{CO} involving the other oxygen atom.

Calculations were performed to obtain estimates of the enthalpies of formation of all the benzodioxoles using appropriate isodesmic reactions. There is a perfect agreement between theoretical and experimental results.

Introduction

Sesame oil contains powerful natural antioxidants (sesamin, sesamol, sesamol and phytosterol) which give the oil very good oxidative stability. Sesamol (5-hydroxy-1,3-benzodioxole) is a natural antioxidant that can prevent the oil being oxidized and losing its distinctive taste, thus, it enhances its storage durability. The antioxidants can explain the reputation of this oil for slowing the ageing process and increasing longevity as certainly regular oiling of the skin restores moisture to the skin, keeping it soft, flexible and young looking.¹

In the experimental part of this paper, we report the standard molar enthalpies of formation, in the condensed and in the gaseous phases, of sesamol (5-hydroxy-1,3-benzodioxole) as well as of other derivatives of 1,3-benzodioxole: piperonyl alcohol (1,3-benzodioxole-5-methanol), piperonylic acid (1,3-benzodioxole-5-carboxylic acid) and homopiperonylic acid (1,3-benzodioxole-5-acetic acid) in the gas phase.



R = OH; CH₂OH, COOH, CH₂COOH

The results of the measurements of combustion energies, using a static bomb calorimeter, and the values for the enthalpies of sublimation of the compounds, derived from the measurement of vapour pressures at different temperatures using the Knudsen effusion technique, were combined to yield the standard molar enthalpies of formation in the gaseous phase.

The most stable geometries of the four compounds were

obtained using density functional theory with the B3LYP functional and two basis sets: 6-31G** and 6-311G**.

In the 1,3-benzodioxole molecule, since no CH₂–CH₂ interactions (responsible for torsional strain) are present, planarity would be expected. However that is not the case as some studies based on the far-infrared, Raman and dispersed fluorescence spectra of both the ground electronic state² and the first excited electronic state³ of 1,3-benzodioxole clearly indicate a preference for puckered-ring conformations. Choo *et al.*,⁴ using a natural bonding orbital (NBO) analysis of the Hartree–Fock wave functions, show that the conformational preference of the puckered conformer over the planar is the result of a wide variety of hyperconjugative orbital interactions, but the interaction between the oxygen lone pair (n_p) and the C–O antibonding orbital (σ^*_{CO}), commonly associated with the anomeric effect, plays a decisive role in explaining nonplanarity. In this work we try to analyze the effect of the substituent R (R = –OH, –CH₂OH, –COOH or –CH₂COOH) in position 5 of 1,3-benzodioxole on the magnitude of the puckering angle.

The values of the gas phase enthalpies of formation, $\Delta_f H_m^\circ(\text{g})$, for the 1,3-benzodioxole derivatives were calculated using appropriate isodesmic reactions. There is a good agreement between calculated and experimental enthalpies of formation.

Results and discussion

Experimental results

The temperature of fusion of each compound was measured using a differential scanning calorimeter. The results (observed at the onset of the calorimetric peaks), T_{fus} , are presented in Table 1 together with the enthalpies of fusion, at the tem-

Table 1 Temperatures of fusion, T_{fus} , enthalpies of fusion, $\Delta_{\text{cr}}^{\text{f}} H_{\text{m}}^{\circ}(T_{\text{fus}})$, and mass fraction of impurities, x , of the studied benzodioxoles

	T_{fus}/K	$\Delta_{\text{cr}}^{\text{f}} H_{\text{m}}^{\circ}(T_{\text{fus}})/\text{kJ mol}^{-1}$	$10^3 \cdot x$
Sesamol	337.74 ± 0.04	16.96 ± 0.02	0.3
Piperonyl alcohol	327.11 ± 0.08	18.05 ± 0.04	0.4
Piperonylic acid	501.58 ± 0.17	30.50 ± 0.19	2.0
Homopiperonylic acid	401.67 ± 0.40	24.94 ± 0.16	1.3

Table 2 Typical combustion experiments, at $T = 298.15 \text{ K}$

	Sesamol	Piperonyl alcohol	Piperonylic acid	Homopiperonylic acid
$m(\text{CO}_2, \text{total})/\text{g}$	1.50236	1.68104	1.91189	1.31232
$m(\text{cpd})/\text{g}$	0.67053	0.72418	0.55945	0.59432
$m'(\text{fuse})/\text{g}$	0.00421	0.00372	0.00388	0.00352
$\Delta T_{\text{ad}}/\text{K}$	0.97269	1.15057	0.71103	0.83123
$\varepsilon_f/(\text{J K}^{-1})$	15.66	16.21	15.30	15.52
$\Delta m(\text{H}_2\text{O})/\text{g}$	0.0	0.0	0.1	0.0
$-\Delta U(\text{IBP})/\text{J}$	15581.74	18432.09	11389.87	13315.39
$\Delta U(\text{fuse})/\text{J}$	68.37	60.41	63.01	57.16
$\Delta U(\text{HNO}_3)/\text{J}$	0.40	0.38	0.11	0.08
$\Delta U(\text{ign.})/\text{J}$	1.20	1.20	1.20	1.18
$\Delta U_{\text{f}}/\text{J}$	12.08	12.81	10.01	10.43
$-\Delta_{\text{cr}}^{\text{f}} H_{\text{m}}^{\circ}/(\text{J g}^{-1})$	23117.37	25350.73	20228.33	22290.55

Table 3 Individual values of the massic energy of combustion, at $T = 298.15 \text{ K}$

$-\Delta_{\text{c}}t^{\text{o}}/(\text{J g}^{-1})$			
Sesamol	Piperonyl alcohol	Piperonylic acid	Homopiperonylic acid
23125.07	25374.48	20237.24	22325.08
23142.65	25349.42	20234.73	22290.55
23125.37	25350.73	20240.96	22304.05
23112.18	25335.63	20220.10	22286.67
23117.37	25346.04	20212.38	22294.51
23122.09	25364.74	20228.33	22296.15
23148.35	25360.36		
23113.18	25347.84		
$-\langle \Delta_{\text{c}}t^{\text{o}} \rangle/(\text{J g}^{-1})$			
23125.7 ± 4.7	25353.7 ± 4.3	20229.0 ± 4.5	20299.5 ± 5.6

peratures of fusion, $\Delta_{\text{cr}}^{\text{f}} H_{\text{m}}^{\circ}(T_{\text{fus}})$, and the mass fraction of impurities, x , of the purified samples.

Results for a typical combustion experiment of each compound are given in Table 2, where $\Delta m(\text{H}_2\text{O})$ is the deviation of the mass of water added to the calorimeter from 3119.6 g. Combustion experiments were carried out in oxygen at $p = 3.04 \text{ MPa}$, with 1.00 cm^3 of water added to the bomb: ΔU_{f} is the correction to the standard state. The remaining quantities are as previously described.⁵ For the cotton-thread fuse, empirical formula $\text{CH}_{1.686}\text{O}_{0.843}$, $\Delta_{\text{cr}}^{\text{f}} H_{\text{m}}^{\circ} = -16250 \text{ J g}^{-1}$,⁶ this value has been confirmed in our laboratory. The corrections for nitric acid formation $\Delta U(\text{HNO}_3)$ were based on $-59.7 \text{ kJ mol}^{-1}$,⁷ for the molar energy of formation of $0.1 \text{ mol dm}^{-3} \text{ HNO}_3(\text{aq})$ from N_2 , O_2 , and $\text{H}_2\text{O}(\text{l})$. As samples were ignited at $T = 298.15 \text{ K}$,

$$\Delta U(\text{IBP}) = -\{\varepsilon_{\text{cal}} + \Delta m(\text{H}_2\text{O}) \cdot c_p(\text{H}_2\text{O}, \text{l}) + \varepsilon_{\text{f}}\} \Delta T_{\text{ad}} + \Delta U_{\text{ign}} \quad (1)$$

where $\Delta U(\text{IBP})$ is the energy associated with the isothermal bomb process, ε_{f} is the energy of the bomb contents after ignition and ΔT_{ad} is the adiabatic temperature rise. The individual results of all combustion experiments, together with the mean value and its standard deviation, are given for each compound in Table 3. Table 4 lists the derived standard molar energies and enthalpies of combustion, $\Delta_{\text{c}} U_{\text{m}}^{\circ}(\text{cr})$ and $\Delta_{\text{c}} H_{\text{m}}^{\circ}(\text{cr})$, and the standard molar enthalpies of formation for the compounds in crystalline phase $\Delta_{\text{f}} H_{\text{m}}^{\circ}(\text{cr})$ at $T = 298.15 \text{ K}$. In accordance with customary thermochemical practice, the uncertainties assigned to the standard molar enthalpies of combustion are, in each case, twice the overall standard

deviation of the mean and include the uncertainties in calibration⁸ and in the values of auxiliary quantities. To derive $\Delta_{\text{f}} H_{\text{m}}^{\circ}(\text{cr})$ from $\Delta_{\text{c}} H_{\text{m}}^{\circ}(\text{cr})$ the standard molar enthalpies of formation of $\text{H}_2\text{O}(\text{l})$ and $\text{CO}_2(\text{g})$, at $T = 298.15 \text{ K}$, $-(285.830 \pm 0.042) \text{ kJ mol}^{-1}$ and $-(393.51 \pm 0.13) \text{ kJ mol}^{-1}$,⁹ respectively, were used.

The integrated form of the Clausius–Clapeyron equation, $\ln(p/\text{Pa}) = a - b \cdot (\text{K}/T)$, where a is a constant and $b = \Delta_{\text{cr}}^{\text{f}} H_{\text{m}}^{\circ}(\langle T \rangle)/R$, was used to derive the standard molar enthalpies of sublimation at the mean temperature of the experimental temperature range. The experimental results obtained from each effusion cell and for each studied compound, together with the residuals of the Clausius–Clapeyron equation, derived from least squares adjustment, are presented in Table 5. For each substance the calculated enthalpies of sublimation obtained from each individual orifice are in agreement within experimental error. The entropies of sublimation at equilibrium conditions were calculated as

$$\Delta_{\text{cr}}^{\text{f}} S_{\text{m}}\{\langle T \rangle, p(\langle T \rangle)\} = \Delta_{\text{cr}}^{\text{f}} H_{\text{m}}^{\circ}(\langle T \rangle)/\langle T \rangle.$$

Table 6 presents, for each orifice used and for the global treatment of all the (p, T) points obtained for each studied compound, the detailed parameters of the Clausius–Clapeyron equation together with the calculated standard deviations and the standard molar enthalpies of sublimation at the mean temperature of the experiments $T = \langle T \rangle$. The equilibrium pressure at this temperature $p(\langle T \rangle)$ and the entropies of sublimation at equilibrium conditions are also presented. The plots of $\ln p = f(1/T)$ for the global results obtained for each

Table 4 Derived standard ($p^\circ = 0.1$ MPa) molar values, at $T = 298.15$ K

	$-\Delta_c U_m^\circ(\text{cr})/\text{kJ mol}^{-1}$	$-\Delta_c H_m^\circ(\text{cr})/\text{kJ mol}^{-1}$	$-\Delta_c H_m^\circ(\text{cr})/\text{kJ mol}^{-1}$
Sesamol	3194.2 ± 1.5	3194.2 ± 1.5	417.9 ± 1.8
Piperonyl alcohol	3857.5 ± 1.6	3858.7 ± 1.6	432.7 ± 1.9
Piperonylic acid	3360.7 ± 1.6	3359.5 ± 1.6	646.1 ± 1.9
Homopiperonylic acid	4017.5 ± 2.2	4017.5 ± 2.2	667.4 ± 2.5

Table 5 Knudsen effusion results for the compounds studied. The vapour pressures obtained from each hole are denoted by p , and the deviations of the experimental results from those given by the Clausius–Clapeyron equations are denoted by $\Delta \ln(p/\text{Pa})$

T/K	t/s	p/Pa			$\Delta \ln(p/\text{Pa})$		
		orifice 1	orifice 2	orifice 3	orifice 1	orifice 2	orifice 3
Sesamol							
293.22	21940	0.139	0.138	0.134	1.9	2.0	1.2
297.08	17527	0.218	0.216	0.216	−1.6	−2.2	−0.2
299.19	15528	0.291	0.290	0.277	0.9	1.0	−2.0
301.17	14834	0.362	0.357	0.359	−1.4	−2.7	−0.5
303.14	10106			0.468	—	—	2.1
305.19	11006	0.588	0.605	0.580	−1.1	1.5	−1.1
307.14	10596	0.735	0.750	0.736	−1.8	−0.1	−0.3
309.14	10826	0.975	0.953	0.942	3.3	0.5	0.9
Piperonyl alcohol							
305.14	21905	0.210	0.205	0.211	−1.0	−2.6	−0.5
307.17	24125	0.277	0.280	0.280	−0.3	1.4	1.3
309.15	20772	0.370	0.365	0.363	2.9	2.1	1.7
311.16	11251	0.462	0.430	0.451	−0.7		−2.4
313.22	15199	0.570	0.604	0.592		0.1	−1.4
315.17	12754	0.751	0.759	0.761	−2.9	−1.5	−0.5
317.14	13838	1.01	1.00	0.993	2.3	2.0	1.8
319.18	12306	1.26	1.25	1.25	−0.4	−1.5	0.0
Piperonylic acid							
363.22	21795	0.217	0.223	0.213	−2.6	0.3	−1.3
365.18	21638	0.276	0.267	0.266	1.2	−1.9	0.4
367.17	19823	0.330	0.330	0.324	−1.0	−0.9	−0.3
369.19	18445	0.413	0.408	0.401	1.0	0.1	0.6
371.15	16238	0.512	0.511	0.492	3.0	3.3	1.5
373.15	11005	0.618	0.617	0.601	2.2	2.5	1.5
375.16	10855	0.729	0.717	0.709	−0.9	−2.0	−1.6
377.35	11367	0.884	0.889	0.885	−2.8	−1.5	−0.8
Homopiperonylic acid							
345.79	23857	0.122	0.116		−0.2	−1.7	
347.00	23144		0.134	0.131		−1.7	−3.5
349.81	22726	0.197	0.197	0.195	0.8	3.1	2.7
352.19	21829	0.260	0.258	0.252	0.7	1.6	0.5
354.93	18526	0.352	0.351	0.348	−0.2	0.5	0.9
357.20	15088	0.449	0.449	0.454	−1.2	−1.1	1.6
360.13	12408	0.614		0.611	−2.5		−1.5
362.80	24194	0.869	0.866	0.848	3.1	1.4	1.7
364.01	13440	0.954	0.958	0.929	−0.6	−2.0	−2.5

compound are presented in Fig. 1. Equation 2 was used to derive the sublimation enthalpies at the temperature 298.15 K from the sublimation enthalpies calculated at the mean temperature $\langle T \rangle$ of the experiments:

$$\Delta_{\text{cr}}^{\text{g}} H_m^\circ(T = 298.15 \text{ K}) = \Delta_{\text{cr}}^{\text{g}} H_m^\circ(\langle T \rangle) + \Delta_{\text{cr}}^{\text{g}} C_{p,m}^\circ(298.15 \text{ K} - \langle T \rangle). \quad (2)$$

As no experimental heat capacity data were found, the value $\Delta_{\text{cr}}^{\text{g}} C_{p,m}^\circ = -(50 \pm 20) \text{ J K}^{-1} \text{ mol}^{-1}$ was estimated for the studied compounds.¹⁰

The enthalpies of sublimation of the studied acids are considerably larger than the enthalpies of sublimation of the related alcohols:

$$\begin{aligned} \Delta\{\Delta_{\text{cr}}^{\text{g}} H_m^\circ, \text{piperonylic acid}\} - \{\Delta_{\text{cr}}^{\text{g}} H_m^\circ, \text{sesamol}\} &= 25 \text{ kJ mol}^{-1} \\ \Delta\{\Delta_{\text{cr}}^{\text{g}} H_m^\circ, \text{homopiperonylic acid}\} - \\ &\quad \{\Delta_{\text{cr}}^{\text{g}} H_m^\circ, \text{piperonyl alcohol}\} = 19 \text{ kJ mol}^{-1} \end{aligned}$$

The differences between those values are a consequence of the strong intermolecular attractions between the acid molecules which are packed as hydrogen bonded dimers in the crystals. A similar difference (20 kJ mol^{-1}) is found when comparing the enthalpies of sublimation of benzoic acid {recommended value¹¹ $\Delta_{\text{cr}}^{\text{g}} H_m^\circ = (89.7 \pm 1.0) \text{ kJ mol}^{-1}$ } and phenol { $\Delta_{\text{cr}}^{\text{g}} H_m^\circ = (69.7 \pm 0.9) \text{ kJ mol}^{-1}$ }¹²}.

The standard molar enthalpies of sublimation and of formation, in both the condensed and gaseous phases, at the temperature 298.15 K for the studied compounds are summarized in Table 7.

Theoretical results

Optimized geometries

The geometries of all molecules have been fully optimized and the resulting most relevant geometrical parameters are

Table 6 Experimental results for the studied compounds where a and b are from Clausius–Clapeyron equation $\ln(p/\text{Pa}) = a - b \cdot (K/T)$, $b = \Delta_{\text{cr}}^{\text{g}} H_{\text{m}}^{\circ} / (R \cdot T)$; $R = 8.3145 \text{ J K}^{-1} \text{ mol}^{-1}$

Hole number	a	b	$\langle T \rangle / \text{K}$	$p(\langle T \rangle) / \text{Pa}$	$\Delta_{\text{cr}}^{\text{g}} H_{\text{m}}^{\circ} (\langle T \rangle) / \text{kJ mol}^{-1}$	$\Delta_{\text{cr}}^{\text{g}} S_{\text{m}}^{\circ} \{ \langle T \rangle, p(\langle T \rangle) \} / \text{J K}^{-1} \text{ mol}^{-1}$
Sesamol						
1	35.59 ± 0.47	11019 ± 143			91.6 ± 1.2	
2	35.85 ± 0.42	11100 ± 127			92.3 ± 1.1	
3	35.90 ± 0.30	11121 ± 92			92.5 ± 0.8	
global	35.77 ± 0.24	11078 ± 72	301.18	0.364	92.1 ± 0.6	305.8 ± 2.0
Piperonyl alcohol						
1	39.11 ± 0.53	12407 ± 164			103.2 ± 1.4	
2	39.21 ± 0.50	12440 ± 156			103.4 ± 1.3	
3	38.83 ± 0.39	12322 ± 123			102.4 ± 1.0	
global	39.05 ± 0.25	12389 ± 78	312.16	0.528	103.0 ± 0.6	330.0 ± 1.9
Piperonylic acid						
1	36.08 ± 0.67	13651 ± 247			113.5 ± 2.0	
2	35.89 ± 0.61	13582 ± 227			112.9 ± 1.9	
3	36.85 ± 0.37	13758 ± 136			114.4 ± 1.1	
global	36.11 ± 0.35	13664 ± 130	370.28	0.453	113.6 ± 1.1	306.8 ± 3.0
Homopiperonylic acid						
1	39.08 ± 0.37	14241 ± 132			118.4 ± 1.1	
2	40.15 ± 0.40	14625 ± 143			121.6 ± 1.2	
3	39.67 ± 0.53	14458 ± 187			120.2 ± 1.6	
global	39.64 ± 0.27	14444 ± 95	354.90	0.347	120.1 ± 0.8	338.4 ± 2.2

Table 7 Derived standard ($p^{\circ} = 0.1 \text{ MPa}$) molar values of the enthalpies of formation in the gas phase, at $T = 298.15 \text{ K}$

	$-\Delta_{\text{f}} H_{\text{m}}^{\circ} (\text{cr}) / \text{kJ mol}^{-1}$	$\Delta_{\text{cr}}^{\text{g}} H_{\text{m}}^{\circ} / \text{kJ mol}^{-1}$	$-\Delta_{\text{f}} H_{\text{m}}^{\circ} (\text{g}) / \text{kJ mol}^{-1}$
Sesamol	417.9 ± 1.8	92.2 ± 0.6	325.7 ± 1.9
Piperonyl alcohol	432.7 ± 1.9	103.7 ± 0.7	329.0 ± 2.0
Piperonylic acid	646.1 ± 1.9	117.2 ± 1.8	528.9 ± 2.6
Homopiperonylic acid	667.4 ± 2.5	122.9 ± 1.4	544.5 ± 2.9

Table 8 Calculated B3LYP/6-311G** bond angles ($^{\circ}$) and bond lengths (\AA)

	θ_{2145}	θ_{6321}	$\theta_{1110 \text{ } 8 \text{ } 7}$	$\text{O}_1\text{--C}_2$	$\text{O}_1\text{--C}_5$	$\text{C}_3\text{--O}_4$	$\text{O}_4\text{--C}_5$	$\text{C}_8\text{--R}$	$\text{C}_2\text{--C}_3$	$\text{C}_3\text{--C}_6$	$\text{C}_6\text{--C}_7$	$\text{C}_7\text{--C}_8$	$\text{C}_8\text{--C}_9$	$\text{C}_2\text{--C}_9$
Benzodioxole	13.3	1.2	—	1.375	1.433	1.375	1.433	—	1.391	1.378	1.405	1.391	1.405	1.378
Sesamol	15.2	1.3	0.0	1.371	1.435	1.379	1.429	1.370	1.392	1.374	1.407	1.393	1.407	1.376
Piperonyl alcohol	17.2	2.2	36.7	1.376	1.431	1.375	1.432	1.510	1.392	1.377	1.405	1.394	1.409	1.376
Piperonylic acid	9.5	1.0	0.0	1.372	1.431	1.364	1.438	1.482	1.395	1.379	1.400	1.397	1.412	1.372
Homopiperonylic acid	16.4	1.4	64.3	1.373	1.432	1.373	1.433	1.520	1.393	1.376	1.406	1.393	1.411	1.375

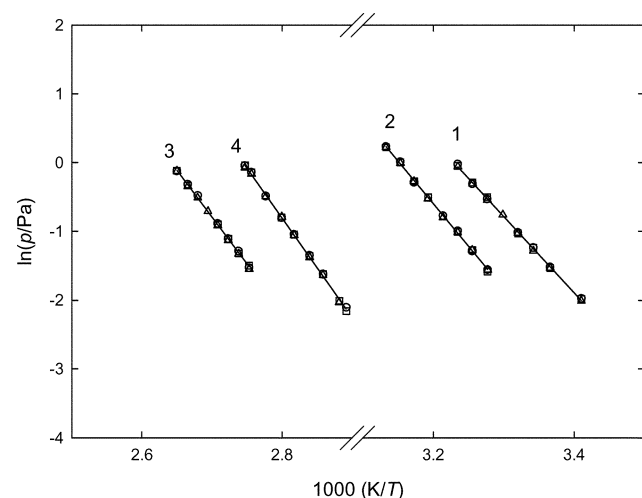


Fig. 1 Plots of $\ln(p/\text{Pa})$ against $1/T$ for the studied compounds: 1, sesamol; 2, piperonyl alcohol; 3, piperonylic acid; 4, homopiperonylic acid. \circ , orifice 1; \square , orifice 2; Δ , orifice 3.

displayed in Table 8. Figure 2 shows the atom numbering scheme used.

The most interesting feature of the studied systems at their

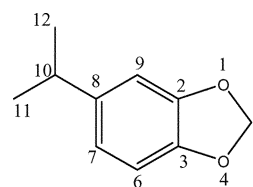


Fig. 2 Atom numbering scheme for the geometric results of the benzodioxole derivatives.

most stable conformations is a variable degree of ring puckering (angle θ_{2145} , see Fig. 2) and an essentially null tendency to exhibit ring flapping (angle θ_{6321}). The observed ring-puckering tendency has been attributed¹³ to the anomeric effect, which occurs in systems with O–C–O linkages. The analysis of the importance of anomeric (hyperconjugative) orbital interactions can be appropriately done by Natural Bond Orbital¹⁴ (NBO) calculations as shown in previously reported studies of 1,3-dioxole,¹⁵ 1,3-benzodioxole,⁴ phthalan,¹⁶ substituted 1,3-dioxane and 1,3-dithiane,¹⁷ 2,4-dioxahexane and 2,4,6-trioxahexane.¹⁸

In the framework of the NBO method the canonical molecular orbitals are transformed into a set of localized hybrids (NBOs) described in terms of an orthogonalized atomic orbital basis set. The resulting filled NBOs describe covalency effects in

the molecules while small occupancies of the nominally unoccupied antibonding NBOs are used to describe departures from an idealized Lewis picture and thus represent small noncovalency corrections to the picture of localized covalent bonds. The energy associated with such effects can be numerically assessed by deleting the relevant NBOs from the bond set and recalculating the total energy, thus determining the associated variational energy lowering. In this way the total energy can be broken down into components associated with the covalent and selected non-covalent contributions. Deletion of all the virtual NBOs similarly leads to estimates of the overall effect of electron delocalization (ϵ_{del}).

In order to analyze the effect of hyperconjugative orbital interactions on the amount of ring puckering of the most stable conformations of these systems we have optimized the corresponding planar structures (by restricting the angle θ_{2145} to 0°) and then we have performed NBO analyses for both conformations. Our results indicate that the observed variable degrees of ring puckering for the equilibrium structures of the studied molecules result from the relative balance of a large number of individual interactions leading to opposite forces: those favoring a puckering of the pentagonal ring and those that favor the corresponding planar conformation. It is observed from the values of the delocalization energy differences ($\Delta\epsilon_{\text{del}}$) between the puckered and the planar conformations (Table 9) that the interactions favoring the puckering of the pentagonal ring are, in all cases, collectively more important than those favoring the planar conformation, thus explaining the larger stability of the puckered conformations.

In addition, a more detailed analysis of individual orbital interactions reveals, as in previous studies of 1,3-dioxole¹⁴ and of 1,3-benzodioxole,⁴ that the most important forces favoring ring puckering are those associated with the interaction of each oxygen atom p lone electronic pair, n_p , with the antibonding C–O orbital, σ^*_{CO} , involving the other oxygen atom ($n_p \rightarrow \sigma^*_{\text{CO}}$), an interaction commonly recognized as describing the so called anomeric effect while, among the forces favoring ring planarity, the interaction between the same oxygen lone electronic pairs and the antibonding C–C π orbitals of the benzenic ring ($n_p \rightarrow \pi^*_{\text{CC}}$) plays a major role. The last interactions tend to establish an extended delocalized π electron system involving the two rings. Table 9 shows the results for both interactions in the puckered and in the planar conformations of all systems, as well as the same interactions for non-substituted benzodioxole in puckered conformations with the same puckering angle as the substituted systems.

On the other hand, when we analyze the values of the variation of the interaction energy for these interactions between the puckered and the planar conformations (columns under Δ in Table 9) we can conclude that the interaction favoring puckered conformations clearly overshadows the interaction favoring planar conformations. In addition the effect of the substituents R is to reinforce both the $n_p \rightarrow \sigma^*_{\text{CO}}$ and the $n_p \rightarrow \pi^*_{\text{CC}}$ energy differences between the puckered and planar conformations, the only exception occurring for the COOH substituent. The variation in these interaction energy differences, rather than being merely the result of the different puckering angles adopted by the systems, seems to be the main factor determining the particular conformations, as can be concluded from a comparison of the interaction energies in substituted benzodioxoles and in non-substituted benzodioxole at the same corresponding puckering angles. Indeed we can observe from the results (columns 3 to 6 of Table 9) that the effect of the substituents R is to reinforce differently both the $n_p \rightarrow \sigma^*_{\text{CO}}$ and $n_p \rightarrow \pi^*_{\text{CC}}$ interactions, when compared with non-substituted benzodioxole. The only exceptions to this behavior are piperonylic acid, for which the $n_p \rightarrow \sigma^*_{\text{CO}}$ is clearly weakened by the substituent and piperonylic alcohol where the substituent has essentially no effect on the $n_p \rightarrow \pi^*_{\text{CC}}$ inter-

Table 9 Variation of delocalization energies between puckered and planar conformations of 1,3-benzodioxole-5-R, $\Delta\epsilon_{\text{del}}$, and main hyperconjugative contributions, $n_p \rightarrow \sigma^*_{\text{CO}}$ and $n_p \rightarrow \pi^*_{\text{CC}}$ (kJ mol^{-1})

1,3-Benzodioxole in the conformation of the 1,3-benzodioxole-5-R	$\Delta\epsilon_{\text{del}}$			Puckered conformation			Planar conformation			$\Delta = \text{Puckered} - \text{Planar}$		
	$n_p \rightarrow \sigma^*_{\text{CO}}$	$n_p \rightarrow \pi^*_{\text{CC}}$	$n_p \rightarrow \sigma^*_{\text{CO}}$	$n_p \rightarrow \sigma^*_{\text{CO}}$	$n_p \rightarrow \pi^*_{\text{CC}}$	$n_p \rightarrow \pi^*_{\text{CC}}$	$n_p \rightarrow \sigma^*_{\text{CO}}$	$n_p \rightarrow \pi^*_{\text{CC}}$	$n_p \rightarrow \pi^*_{\text{CC}}$	$n_p \rightarrow \sigma^*_{\text{CO}}$	$n_p \rightarrow \pi^*_{\text{CC}}$	$n_p \rightarrow \pi^*_{\text{CC}}$
Benzodioxole (R = H)	5.0	188.6	5.0	188.6	188.6	188.6	0	191.3	5.0	5.0	191.3	-2.7
Sesamol (R = OH)	6.3	187.3	6.7	188.4	188.4	188.4	0	192.3	6.7	6.7	192.3	-3.9
Piperonylic alcohol (R = CH_2OH)	7.1	186.3	8.3	186.3	186.3	186.3	0	191.4	8.3	8.3	191.4	-5.1
Piperonylic acid (R = COOH)	3.1	190.4	2.4	201.0	201.0	201.0	0	201.5	2.4	2.4	201.5	-0.5
Homopiperonylic acid (R = CH_2COOH)	6.8	186.6	7.5	190.9	190.9	190.9	0	195.6	7.5	7.5	195.6	-4.7

Table 10 Calculated electronic energies (hartree) and thermal corrections, E_{total} (kJ mol⁻¹)

Compound	$E_{\text{B3LYP/6-31G**}}$	$E_{\text{B3LYP/6-311G**}}$	$E_{\text{total/B3LYP/6-31G**}}^a$
Benzodioxole	-420.785961	-420.889175	310.2
Sesamol	-496.003686	-496.130655	324.5
Piperonyl alcohol	-535.311375	-535.447407	400.7
Piperonylic acid	-609.364372	-609.523720	356.7
Homopiperonylic acid	-648.673791	-648.841937	432.1
Methane	-40.524007	-40.534248	121.2
Methanol	-115.723956	-115.758691	138.4
Ethanol	-155.046203	-155.089964	213.7
Acetic acid	-229.091480	-229.159221	168.6
Propanoic acid	-268.406807	-268.485206	244.4
Phenyl formate	-420.808962	-420.916093	309.1

$$^a E_{\text{total}} (T = 298.15 \text{ K}) = E_{\text{trans}} + E_{\text{rot}} + E_{\text{ZP}} + \Delta_{0 \text{ K}}^{298.15 \text{ K}} E_{\text{vib}}$$

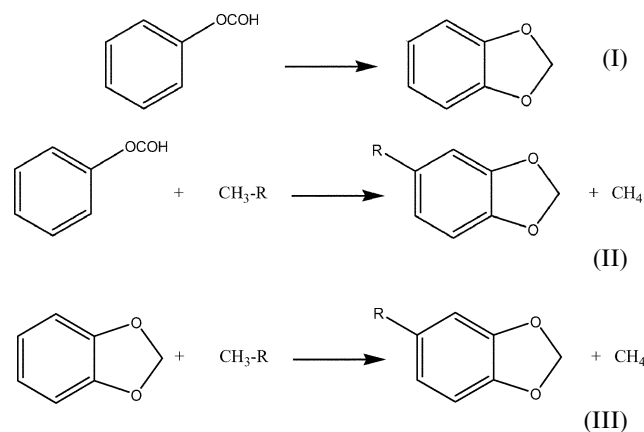
Table 11 Theoretical estimates of the standard enthalpies of formation in the gas phase at $T = 298.15 \text{ K}$ (kJ mol⁻¹) of benzodioxoles

	$\Delta_f H_m^0 \text{ (g)}$			
	Reaction I	Reaction II	Reaction III	Experimental
Benzodioxole	-143.2	—	—	-142.7 ± 2.9 ¹³
Sesamol	—	-317.3	-316.8	-325.7 ± 1.9
Piperonyl alcohol	—	-313.1	-312.6	-329.0 ± 2.0
Piperonylic acid	—	-527.9	-527.4	-528.9 ± 2.6
Homopiperonylic acid	—	-530.8	-530.4	-544.5 ± 2.9

action energy. This behavior results in a considerable reduction of the puckering angle in piperonylic acid (Table 8).

Calculated enthalpies of formation

In order to estimate the enthalpies of formation of the systems from the calculated energies we used the following set of reactions involving auxiliary systems whose thermochemical properties are well established experimentally:¹⁹



These reactions are likely to produce a substantial cancellation of the correlation errors introduced in the calculations since they are of the isodesmic type.

Total energies, identified by the subscripts B3LYP/6-31G**, B3LYP/6-311G**, are reported in Table 10. Energies are given for benzodioxole and the studied 5-derivatives, as well for other auxiliary molecules involved in the isodesmic reactions. The optimum geometries, the energies and the thermal corrections for all auxiliary molecules have also been obtained using the same procedures as described above and the resulting estimates of the enthalpies of formation, at the B3LYP/6-311G**//B3LYP/6-31G** level of calculation, are provided in Table 11.

We can observe from the results in Table 11 that the calculated enthalpies of formation are in good agreement with the experimental data, the average error being only 8.6 kJ mol⁻¹, the worst results being those corresponding to piperonylic

alcohol and homopiperonylic acid with errors of about 16 kJ mol⁻¹ and 13 kJ mol⁻¹, respectively.

Experimental

Materials

All the compounds are commercial products from Aldrich Chemical Co.: sesamol [533-31-3], 99.1% (g.c.), piperonyl alcohol [495-76-1], 99.0% (g.l.c.), piperonylic acid [94-53-1], 99.8% (g.l.c.) and homopiperonylic acid [2861-28-1], 98.4% (g.c.). All the samples were purified by repeated sublimation under reduced pressure before experimental studies. Their impurity mass fractions (Table 1) were derived from d.s.c. (Setaram DSC 141) analysis by a fractional fusion technique.²⁰ The samples, hermetically sealed in stainless steel crucibles, were heated at $3.33 \times 10^{-2} \text{ K s}^{-1}$. The temperature scale of the calorimeter was calibrated by measuring the melting temperature of three high purity reference materials (naphthalene, benzoic acid and indium)¹¹ and its power scale was calibrated with high-purity indium (mass fraction > 0.99999). The recorded thermograms did not show any phase transition between 298 K and the melting temperature of the studied compounds.

The purity of the samples was also confirmed through the carbon dioxide recovery ratios. The average ratios, together with the standard deviation of the mean, of the mass of carbon dioxide recovered to that calculated from the mass of sample were: sesamol (1.0003 ± 0.0002), piperonyl alcohol (1.0002 ± 0.0004), piperonylic acid (0.9994 ± 0.0002) and homopiperonylic acid (1.0001 ± 0.0001). The densities of the samples were estimated as 1.0 g cm^{-3} .

Combustion calorimetry

The combustion experiments were performed with a static bomb calorimeter. The apparatus and technique have been described.^{21,22} Benzoic acid (Bureau of Analysed Samples, Thermochemical Standard, BCS-CRM-190 p) was used for calibration of the bomb. Its massic energy of combustion is $-\Delta_c u = (26432.3 \pm 3.8) \text{ J g}^{-1}$, under certificate conditions. The calibration results were corrected to give the energy equivalent ϵ_{cal} corresponding to the average mass of water added to the

calorimeter, 3119.6 g. From six calibration experiments performed $\varepsilon_{\text{cal}} = (16004.8 \pm 1.6) \text{ J K}^{-1}$, where the uncertainty quoted is the standard deviation of the mean.

Vapour pressure measurements

A mass-loss Knudsen-effusion apparatus enabling the simultaneous operation of three Knudsen cells, with three different effusion orifices, was used to measure the vapour pressures of the purified crystalline samples at several temperatures. A detailed description of the apparatus, procedure and technique has been reported before.²³ The consistency of the vapour pressure results measured with this apparatus was also checked, comparing the results obtained for benzoic acid with the results obtained for this compound using a simultaneous torsion and mass-loss effusion method and two different static methods.²⁴

In a typical effusion experiment the samples are assumed to be in thermal equilibrium with a thermostatically controlled silicone oil bath in which the effusion cells are immersed. The loss of mass Δm of the samples during a convenient effusion time period t is determined by weighing the effusion cells to $\pm 0.01 \text{ mg}$ before and after the effusion period in a system evacuated to a pressure near $1 \times 10^{-4} \text{ Pa}$. At the temperature T of the experiment, the vapour pressure p is calculated by eqn. (3):

$$p = (\Delta m / A_o w_o t) \cdot (2\pi RT / M)^{1/2} \quad (3)$$

where M is the molar mass of the effusing vapour, R is the gas constant, A_o is the area of the effusion orifice and w_o is the respective Clausing factor calculated by eqn. (4):

$$w_o = \{1 + (3l/8r)\}^{-1} \quad (4)$$

where l is the thickness of the effusion orifice and r its radius. In this work, effusion orifices made in platinum foil of 0.0125 mm thickness were used. Their areas and Clausing factors were: orifice 1, $A_o/\text{mm}^2 = 0.663$, $w_o = 0.990$; orifice 2, $A_o/\text{mm}^2 = 0.785$, $w_o = 0.991$; orifice 3, $A_o/\text{mm}^2 = 0.996$, $w_o = 0.992$.

Computational details

The geometries of all molecules have been fully optimized using density functional theory (DFT) with the Becke 3-parameter hybrid exchange²⁵ and the Lee–Yang–Parr²⁶ correlation density functionals (B3LYP) and the Pople's split-valence 6-31G** extended basis set.²⁷ The optimum structures so obtained were further certified as true minima by constructing and diagonalizing the corresponding cartesian hessian matrix, this procedure providing also the harmonic vibrational frequencies which, after being properly scaled by the recommended scaling factor 0.9614,²⁸ allow the reliable calculation of the thermal corrections to the molecular energy. We have further refined the optimum structures by reoptimizing them using the same methodology with the Pople's split-valence 6-311G** extended basis set.²⁷

The NBO analyses have been done on B3LYP/6-31G** wave functions obtained with the B3LYP/6-311G** optimum geometries. All calculations have been performed using the UK version of the program GAMESS.^{29,30}

Acknowledgements

Thanks are due to Fundação para a Ciência e a Tecnologia, F.C.T., Lisbon, Portugal, for financial support to Centro de Investigação em Química of the University of Porto.

References

- 1 <http://www.dagangasia.com/emerchant/eStore15ELS/News.asp?TenantID=186>.
- 2 S. Sakurai, N. Meinander, K. Morris and J. Laane, *J. Am. Chem. Soc.*, 1999, **121**, 5056.
- 3 J. Laane, E. Bondoc, S. Sakurai, K. Morris, N. Meinander and J. Choo, *J. Am. Chem. Soc.*, 2000, **122**, 2628.
- 4 S. Moon, Y. Kwon, J. Lee and J. Choo, *J. Phys. Chem. A*, 2001, **105**, 3221.
- 5 W. N. Hubbard, D. W. Scott, G. Waddington, in *Experimental Thermochemistry: Standard States and Corrections for Combustions in a Bomb at Constant Volume*, ed. F. D. Rossini, Interscience, New York, 1956, Vol. 1, Chap. 5.
- 6 J. Coops, R. S. Jessup, K. Van Nes, in *Experimental Thermochemistry: Calibration of Calorimeters for Reactions in a Bomb at Constant Volume*, ed. F. D. Rossini, Interscience, New York, 1956, Vol. 1, Chap. 3.
- 7 The NBS Tables of Chemical Thermodynamic Properties, *J. Phys. Chem. Ref. Data*, 1982, **11**(Suppl. 2).
- 8 F. D. Rossini, in *Experimental Thermochemistry: Assignment of Uncertainties to Thermochemical Data*, ed. F. D. Rossini, Interscience, New York, 1956, Vol. 1, Chap. 14.
- 9 CODATA, *J. Chem. Thermodyn.*, 1978, **10**, 903.
- 10 Personal communication of J. B. Pedley, University of Sussex, as cited by P. M. Burkinshaw and C. T. Mortimer, *J. Chem. Soc., Dalton Trans.*, 1984, 75. The uncertainty of $\pm (20 \text{ J K}^{-1} \text{ mol}^{-1})$ was assumed in this paper.
- 11 R. Sabbah, A. Xu-wu, J. S. Chickos, M. L. P. Leitão, M. V. Roux and L. A. Torres, *Thermochim. Acta*, 1999, **331**, 93.
- 12 G. H. Parsons, C. H. Rochester and C. E. C. Wood, *J. Chem. Soc. (B)*, 1971, 533.
- 13 E. Cortez, R. Verastegui, J. Villarreal and J. Laane, *J. Am. Chem. Soc.*, 1993, **115**, 12132.
- 14 A. E. Reed, L. A. Curtiss and F. Weinhold, *Chem. Rev.*, 1988, **88**, 899; J. P. Foster and F. Weinhold, *J. Am. Chem. Soc.*, 1980, **102**, 7211; A. E. Reed and F. Weinhold, *J. Chem. Phys.*, 1983, **78**, 4066.
- 15 D. Suárez, L. Sordo and A. Sordo, *J. Am. Chem. Soc.*, 1996, **118**, 9850.
- 16 S. Jeon, J. Choo, S. Kim, Y. Kwon, J. Kim, Y. Lee and H. Chung, *J. Mol. Struct.*, 2002, **609**, 159.
- 17 F. Cortés, J. Tenorio, O. Collera and G. Cuevas, *J. Org. Chem.*, 2001, **66**, 2918.
- 18 C. Cramer, A. Kelterer and A. French, *J. Comput. Chem.*, 2001, **22**, 1194.
- 19 J. B. Pedley, *Thermochemistry Data and Structures of Organic Compounds*, Vol. I, Thermodynamics Research Center, College Station, Texas, USA, 1994.
- 20 C. Plato and A. R. Glasgow, Jr., *Anal. Chem.*, 1969, **41**, 330.
- 21 M. A. V. Ribeiro da Silva, M. D. M. C. Ribeiro da Silva and G. Pilcher, *Rev. Port. Quim.*, 1984, **26**, 163.
- 22 M. A. V. Ribeiro da Silva, M. D. M. C. Ribeiro da Silva and G. Pilcher, *J. Chem. Thermodyn.*, 1984, **16**, 1149.
- 23 M. A. V. Ribeiro da Silva and M. J. S. Monte, *Thermochim. Acta*, 1990, **171**, 169.
- 24 M. A. V. Ribeiro da Silva and M. J. S. Monte, *J. Chem. Thermodyn.*, 1995, **27**, 175.
- 25 A. D. Becke, *J. Chem. Phys.*, 1993, **98**, 5648.
- 26 C. T. Lee, W. T. Yang and R. G. Parr, *Phys. Rev. B*, 1998, **37**, 785.
- 27 P. C. Hariharan and J. A. Pople, *Chem. Phys. Lett.*, 1972, **66**, 217.
- 28 P. A. Scott and L. Radom, *J. Chem. Phys.*, 1996, **100**, 16502.
- 29 UK-GAMESS is a package of *ab initio* programs written by M. F. Guest, J. H. van Lenthe, J. Kendrick, K. Schoffell and P. Sherwood, with contributions from R. D. Amos, R. J. Buenker, H. J. J. van Dam, M. Dupuis, N. C. Handy, I. H. Hillier, P. J. Knowles, V. Bonacic-Koutecky, W. von Niessen, R. J. Harrison, A. P. Rendell, V. R. Saunders, A. J. Stone and A. H. de Vries. The package is derived from the original GAMESS code due to M. Dupuis, D. Spangler and J. Wendoloski, NRCC Software Catalog, Vol. 1, Program No. QG01 (GAMESS), 1980.
- 30 The DFT module within GAMESS-UK was developed by Dr P. Young under the auspices of EPSRC's Collaborative Computational Project No. 1 (CCP1) (1995–1997).